MgO doped Lithium Niobate waveguides based All Optical Modulator

M.Tech. Dissertation submitted to

Malaviya National Institute of Technology Jaipur

Submitted by

Sanjay Kumar Sharma

Institute ID: 2015PWC5344

Under the guidance of

Dr. Ghanshyam Singh

Associate Professor – ECE

In partial fulfillment of project for the award of the degree of

MASTER OF TECHNOLOGY

IN

WIRELESS & OPTICAL COMMUNICATION

Malaviya National Institute of Technology Jaipur

Jaipur, Rajasthan 302017

Department of Electronics and Communication Engineering

Malaviya National Institute of Technology, Jaipur - 302017

CERTIFICATE

This is to certify that the dissertation report **"MgO doped Lithium Niobate waveguides based All Optical Modulator"** composed by **Mr. Sanjay Kumar Sharma (2015PWC5344)**, in the partial fulfilment of the Degree **Master of Technology** in **Wireless and Optical Communication** of Malaviya National Institute of Technology, Jaipur is the work completed by him under my supervision, hence approved for submission during academic session 2016-2017. The contents of this dissertation report, in full or in parts, have not been submitted to any other Institute or University for the award of any degree or diploma.

Place: Jaipur
Date:

Dr. Ghanshyam Singh
Associate Professor, ECE
MNIT jaipur

DECLARTION

I, **Sanjay Kumar Sharma**, declare that this dissertation titled, **"MgO doped Lithium Niobate waveguides based All Optical Modulator"**and the work presented in it is my own. I confirm that:

- This work is done towards the partial fulfilment of the degree of "Master of Technology" at MNIT, Jaipur.
- Where any part of this Dissertation has previously been submitted for a degree or any other qualification at MNIT or any other institution, this has been clearly stated.
- Where I have consulted the published work of others, this is always clearly attributed.
- Where I have quoted from the work of others, the source is always given. With the exception of such quotations, this dissertation is entirely my own work.
- I have acknowledged all main sources of help.

Place: Jaipur
Date

Sanjay Kumar Sharma
2015PWC5344
MNIT jaipur-302017

Acknowledgments

I would like to thank all the people who helped me and inspired me during my research work.

My deepest gratitude goes first to my project supervisor **Dr. Ghanshyam Singh** who expertly guide me and share his great knowledge with me. I also thankful to him for the encouragement and to work with freedom in area of my interest.

I am sincerely thankful to Department of head **Dr. K.K. Sharma** to avail the facilities required for project. Thanks also goes to oral presentation comitee members **Dr. Vijay Janyani** , **Dr. Ritu Sharma** , **Dr. Ravi Maddila** and **Mr. Ashish Kumar Ghunawat** for the and their evaluation and valuable suggestion time to time.

I am also grateful to India–Ukraine inter-governmental science & technology cooperation programme between the MNIT Jaipur (India) and the Lviv National Polytechnique Institute, Lviv (Ukraine): Project sanction no: INT/RUS/UKR/P-15/2015.

Sanjay Kumar Sharma

Abstract

In last few decades Lithium Niobate become an extremely used and a high interest of material for photonic device fabrication and research because of its high electro-optic properties, low loses and linear response to applied electrical field. Optical signal modulation is the basic requirement for optical communication to carry electrical signal in optical domain. In general Lithium Niobate modulator is fabricated by Ti indiffusion or proton exchange process, but all these conventional optical waveguide formation techniques have many problems such as low refractive index contrast, larger mode size and high $V\pi L$. Beside these congruent Lithium Niobate also have a serious issue of "optical damage" of refractive index of waveguide. So here we proposed a modulator structure which is based on MgO doped LN to overcome these limitations.

This thesis dealt with design and simulation analysis of electrooptic waveguide modulator which employ MgO doped LN . Starting chapters are about the brief introduction of electrooptic effect, Lithium Niobate and conventional waveguide formation techniques. The next chapter deal with the photorefractive effect and how MgO doped LN have advantages over the congruent LN in terms of photo refractive damage performance. And the last chapter is all about the design, simulation, performance, results and discussion of the project.

Keywords-Ridge waveguides, Mach-Zehnder interferometer (MZI), MgO doped Lithium Niobate, External modulator.

List of Symbols

Γ Pockels coefficient or the linear electro-optic coefficient

ξ Kerr's coefficient or the quadratic electro-optic coefficient

n refractive index

n_o ordinary refractive index

n_e extra ordinary refractive index

$V\pi$ voltage required to create 180 degree phase shift in between modulator branch

V applied voltage on electrode

d distance between electrodes

λ wavelength of operation

ζ optical confinement factor inside film

β phase constant

V applied voltage on electrode

d distance between electrode

A, B, C, D, E, F sellimier's equation coefficients

Acronym

LN Lithium Niobate

MgO – LN magnesium oxide doped Lithium Niobate

MZI Mach zehender interferometer

MZM Mach zehender modulator

EO electro optic

BPM beam propagation method

FFT fast Fourier transform

List of figures

List of tables

CONTENTS

CHAPTER 1

1 Lithium Niobate background1 and literature review

1.1 Introduction

In last decade data transmission speed grow exponentially and this could be possible because of evolution in optical communication. In spite of such a high data transmission speed demand for much higher data rate also growing every day. As optical data is meaningful only when it carries some information or we can say it is modulated by RF signal or electrical signal. Modulation process is a very essential part of optical communication and due to limitation of internal modulation external modulation become more popular.

Electrooptic MZI modulation is widely used external modulation technique and due to high electrooptic coefficient property Lithium Niobate is intensively used material for waveguide modulator. Hence improvement in Lithium Niobate based waveguide modulator is essential.

1.2 Lithium Niobate

Lithium Niobate crystal is a vital material for optical waveguides, cell phones, piezoelectric sensors, optical modulators and different other linear and non-nonlinear optical operations [1]. It is a compound material made of niobium, lithium, and oxygen, Lithium Niobate has a trigonal geometry class of R3c and 3m point group framework without anti symmetry and show properties of Ferroelectricity, Pockel's impact, piezoelectric impact, photo elasticity and nonlinear optical polarizability. It is a hard no soluble in water having negative uniaxial birefringence dependent on the stoichiometry and temperature of the crystal [2]. It can be operate under the range of 350 and 5200 nm wavelength. Single crystal of LN wafers grown using the Czochralski process after then wafer is cut into different cuts eg. Z-cut, X-cut, Y-cut[3].

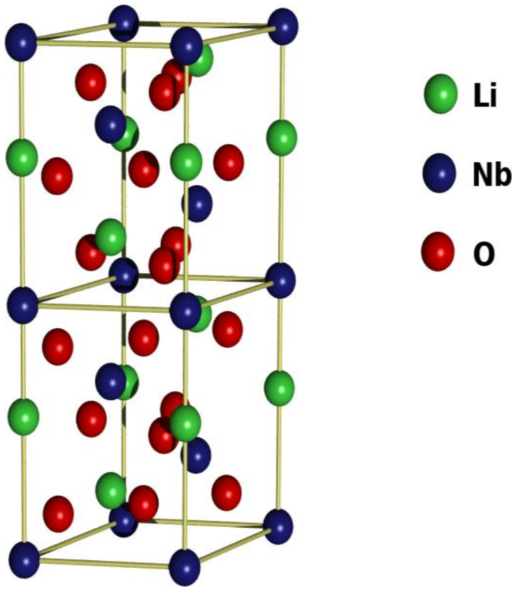

Figure 1.3.1.1Hexagonal unit cell of Lithium Niobate (LiNbO3)[22]

1.3 Electro optic Effect

Some materials show the property by which an optical signal changes its properties according to applied external force. These changes occur due to the change in positions, orientations, or shapes of the molecules constituting the material on applying any external forces eg. Voltage, temperature, acoustic waves etc. [4]. The change in the refractive index resulting from the application of a dc or low-frequency electric field knows as the electro-optic effect .

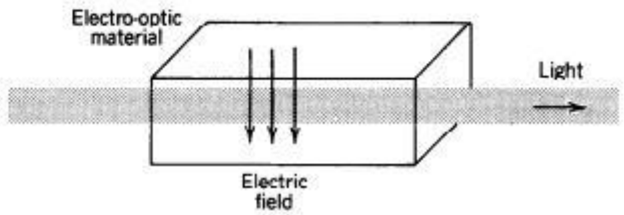

Figure 1.3.1.1 Electrooptic effect

The refractive index of the material can vary in two ways on applying voltage-

(1)The refractive index changes linearly with the applied electric field, the effect is known as the linear electro-optic effect or the Pockel's effect[5].

$$n(E) = \mathrm{n} - \frac{1}{2}\Gamma \mathrm{n}^3\mathrm{E} \qquad (1.3.1)$$

Here Γ is called the Pockels coefficient or the linear electro-optic coefficient, E is applied electric field and n is the refractive index of the medium.

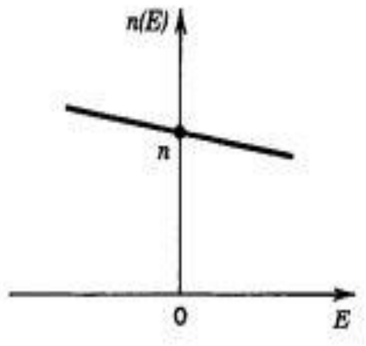

Figure 1.2.2: linear or Pockel EO effect

(2)The refractive index changes in proportion to the square of the applied electric field, the effect is known as the nonlinear electro-optic effect or the Kerr effect[5]

$$n(E) = \mathrm{n} - \frac{1}{2}\xi \mathrm{n}^3\mathrm{E}^2 \qquad (1.3.2)$$

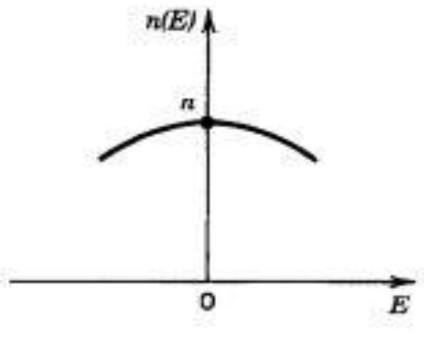

Figure 1.3.1.2Nonlinear or Kerr EO effect

ξ is known as the Kerr coefficient or the quadratic electro-optic coefficient.

1.3.1 Electro optic effect in Lithium Niobate

Lithium Niobate is negative uniaxial crystal having two different refractive index ordinary refractive index (no) and extraordinary refractive index (ne). Lithium Niobate have equal or lower extraordinary refractive (ne) index then its ordinary refractive index (no) which make it birefringent crystal [4,5]. The birefringent property makes Lithium Niobate suitable to use in various integrated optical, electro optical and nonlinear optical applications. Lithium Niobate show electro optic property due to its non-Centro symmetric crystal structure. Lithium Niobate possess a trigonal crystal with the point group symmery3m.refractive index ellipsoid, or indicatrix, is of the Lithium Niobate can be describe as[6,7]

$$\frac{X^2}{n_o^2} + \frac{Y^2}{n_o^2} + \frac{Z^2}{n_e^2} = 1 \qquad (1.3.3)$$

Here n_o and n_e are the ordinary and extraordinary refractive indices respectively, X,Y,Z are the principal die electric axes. When any change occurs in refractive index due applied electric field a corresponding change should be occur in the values of X,Y or Z. New values of principal dielectric axes can be found using a third rank tensor having 27 elements. The tensor for LN in the reduced form can be describe as[8]:

Table 1.5.2.1.1electrooptic tensor of LN

$$r_{ij} = \begin{bmatrix} 0 & -r_{22} & r_{13} \\ 0 & r_{22} & r_{13} \\ 0 & 0 & r_{33} \\ 0 & r_{51} & 0 \\ r_{51} & 0 & 0 \\ -r_{22} & 0 & 0 \end{bmatrix}$$

$r_{22} = -r_{12} = -r_{61} = 3.4$ pm/V,

$r_{33} = 30.8$ pm/V,

$r_{51} = r_{42} = 28$ pm/V.

To maximize the electrooptic effect different kind of crystal cut and different directions of signal propagation used and then according to cut and direction of signal propagation electro optic tensor is used. In OptiBPM simulator software we can choose electro optic tensor according to following table:

Table 1.5.2.1.2 use of electrooptic coefficients depending on the crystal cut and direction of propagation in OptiBPM [9]

		TE mode	TE mode	TM mode	TM mode
Crystal cut	Propagation direction	Horizontal electrode field	Vertical electrode field	Horizontal electrode field	vertical electrode field
X	Y	r_{33}	0	r_{13}	0
Y	X	r_{33}	0	r_{13}	r_{22}
Z	X	r_{22}	r_{13}	0	r_{33}
Z	Y	0	r_{13}	0	r_{33}
Y	Z	0	$-r_{22}$	0	r_{22}
X	Z	r_{22}	0	$-r_{22}$	0

1.4 Optical waveguide formation in Lithium Niobate

Lithium Niobate is one of extensively used material for optical waveguide formation conventional methods used are for optical waveguides in lithium Niobate are: (1) ion-implantation, (2) proton- exchange and, (3) titanium- indiffusion

1.4.1 Ion- Implantation

Ion- implantation is a popular way for the fabrication of optical Waveguides in Lithium Niobate. In the process of ion implantation Substrates is exposed by high energy radiation contain swift heavy ion (SHI) eg. He+,H^+, C+, O+ , Ar4+ etc.

Radiation of heavy ions form buried layer with lower refractive index in the substrate which act as guiding layer and rest of the substrate as cladding media. The depth of the penetration of ion measured by the radiation energy level and the decrement of the refractive index of the LN substrate [10].

Ion implantation is a very efficient and controllable method to change the optical properties near the surface region of LN substrate. The first stage of implantation process is done at lower temperature about 00°C to 220°C known as annealing which remove the ion induced damage from guiding structure and reduce both scattering and propagation losses[11]. After the first stage ion with high energy about 10keV/amu, is bombarded on the structure which alter the refractive index profile of substrate. Decrement in refractive index can be up to 5% depending on ion doses. Process of ion implantation in Lithium Niobate also simultaneously reduce the electrooptic coefficient of the LN substrate [12].

1.4.2 Proton- Exchange

Proton exchange (PE) is a low-cost and widely used technology fabricating optical devices in Lithium Niobate bulk material. It was introduced by Jackel et al. as a means of of producing' the compounds Hydrogen Niobate (HNbO3) and hydrogen tantalite (HTaO3) from Lithium Niobate and Lithium Tantalate, respectively. Proton exchange process completed by a chemical reaction of between Lithium Niobate and an acid (most widely used acid for proton- exchange is benzoic acid (C6H 5CO 2H)) which exchange the Lithium ions from substrate and hydrogen ions from acid over a temperatures range between 15000 and 25000, the depth of the waveguide depend on the time period of the chemical reaction. This process convert the rhombohedral LN structure to the cubic Hydrogen Niobate structure (3 6,3 r). The exchange between the ions allow to form the thin layer over the substrate surface region with increased extraordinary refractive index [13]. The process create the step index varying profile near the surface region [14]. Some post fabrication annealing and dilute melts(when lithium benzoate (C6H5CO2Li) is added to the , benzoic acid known as dilute melts) process are used with ion implantation process to counter balance the high propagation loss,time varying refractive effective mode indices and scattering problems.

1.4.3 Titanium- Indiffusion

The Titanium diffused waveguides in Lithium Niobate waveguides, are framed by the insertion of the Titanium dopant using the diffusion process into the Lithium Niobate. To make a waveguide, a stripe of Titanium is placed on surface of the Lithium Niobate crystal substrate. Ti strip thickness and the width of the Lithium Niobate substrate over which diffusion have to take place is the important factor in waveguide formation. In the process of Ti diffusion [15] first the samples is warmed at the temperature range of hundred to thousand for a time period of some hours. During this period the guest Ti^{+3} replace the host Li^{+} 3 ions gradually and make a reviewed list waveguide, this waveguide has a chime molded refractive index profile along the horizontal and lateral depth and because LN crystal is an anisotropic material so the refractive index variation also depend on the crystal cut and the propagation direction of light. The diffusion of Ti result increment both in ordinary and extraordinary refractive index [16] hence for diffusion of Ti with proper doping concentration can support both TE and TM modes of operation. Beside all the facts Ti diffusion also allow to take advantages of excellent electro-optic, acousto-optic and transmission characteristic of Lithium Niobate and provide good controllability in waveguide fabrication [17].

In above described techniques each have their own merits and demerits and any of the techniques can be use according to application requirements and availability of waveguide fabrication resources. All these conventional techniques is not very much suitable because of low refractive index contrast, larger mode size with very large push pull MZI arm length resulted very high $V\pi L$. To overcome these limitations ridge waveguide modulator structure that employ Lithium Niobate on insulator [18] showing in figure 1(a) have been widely used. Recently Shilei Jin, LongtaoXu et al. [19] proposed ridge waveguide modulator structure having Lithium Niobate thin film and ridge of silicon nitride which show $V\pi L$~3v.cm. Undoped Lithium Niobate shows “optical damage” of photorefractive index while carrying high power which is obvious in WDM system [20]. This problem can be severe, if the device is being use for optical switching therefore suppression of optical damage becomes an important task. Recent studies shows, that doping of MgO in Lithium Niobate (MgO-LN) can help in reducing "optical damage" in refractive index besides that, Doping of MgO also increases the electro-optic constant of Lithium Niobate [21,27].

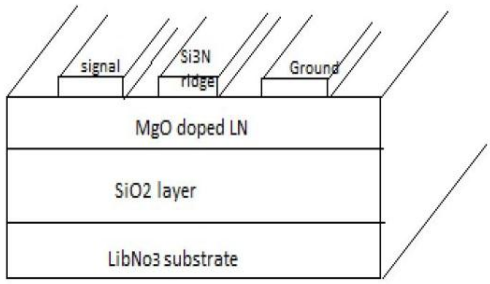

Figure 1.4.3.1 ridge waveguide based optical modulator [41]

1.5 MgO doped Lithium Niobate

1.5.1 Photorefractive effect in congruent Lithium Niobate

Congruent LiNbO3 consist deep and shallow electron traps[21] which originates iron ions Fe2+ and bipolarons NbLi4+Nb Nb4+ sites and small polaronsNbLi4+ sites work as the shallow traps[22]. Such polarons affect the performance of Lithium Niobate adversely. Since pairing to the lattice section firmly extinguishes the tunneling of free small polarons when all is said in done, they are effortlessly confined at one site indeed, even by frail anomalies of Lithium Niobate crystal. The component of their optical ingestions is in this manner imparted to those of small polarons confined by authoritative to choose deserts. It is demonstrated that the optical properties of free electrons in LN and additionally those bound to NbLi antisite deformities can be ascribed reliably to small polarons. The concept is extended to electron sets framing bipolarons bound to NbLi–NbNb closest neighbors in the LN ground state. On the premise of a basic phenomenological approach, depending on commonplace ideas of imperfection material science, the pinnacle energies, line shapes, widths of the related optical assimilation groups and additionally the deformity restricting energies incited by lattice section cause the behave super linear behavior of the Lithium Niobate for the change of photorefractive index during the operation[23].

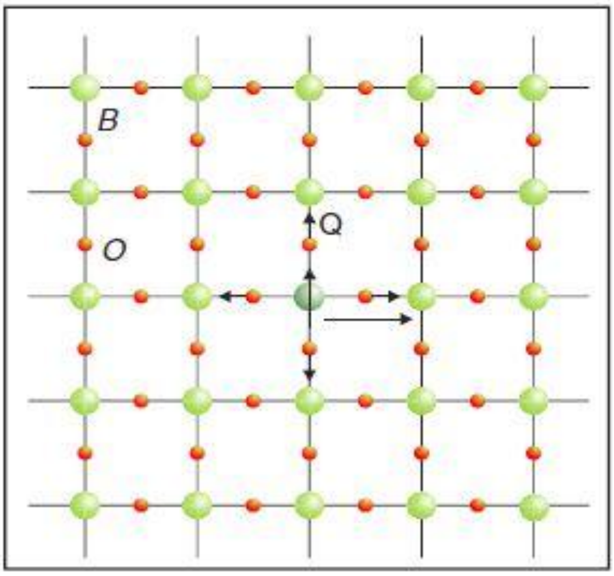

Figure 1.5.1.1small polaron mechanism[23]

Perception of a small electron polaron, self-restricted at a B cation in a BO plane of an ABO3 perovskite. The additional electron, symbolized by its up turn, is balanced out by repulsion essentially of its neighboring particles, depicted by the arranged Q coordination. The electron density is kept around unity For a small polaron. cation site and the cross section bending does not develop more distant than around one bond length. Optical transfer of electron to neighboring cation site which occur with highest probability also cause optical absorption. This is symbolized by the long arrow. Normally the rearranging supposition is made that the electron energy at the last site is definitely not influenced by the distortion at the underlying one.

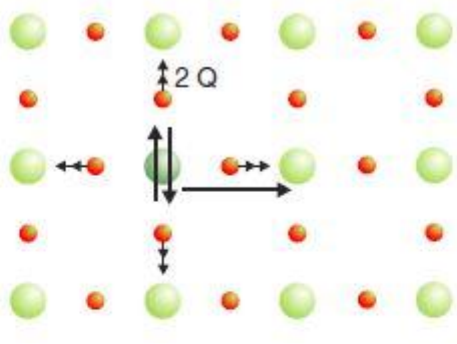

Figure 1.5.1.2small polaron mechanism[23]

The optical absorption in such type of polarons occurs due the transfer of electron , when one of the two electron available in the bipolarons get transferred to other equivalent final cation site represented by a long arrow which leaving only single polarons at original site. The bi polarons after the electron get transferred now adjust itself to as a single polarons. It means that some energy lost absorbed in dissociation pf bipolarons in two single polarons[23,24].

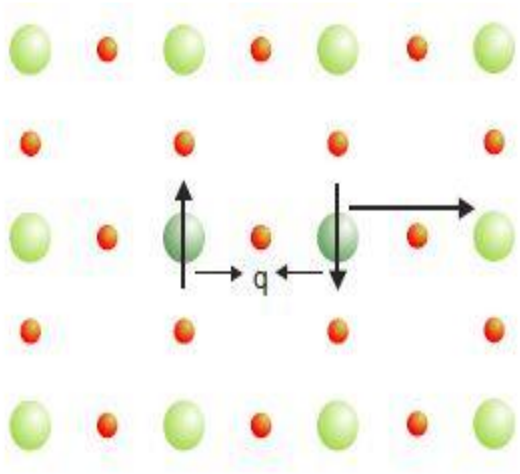

Figure 1.5.1.3Model of a two-site bipolaron[23]

As above figure showing only the necessary displacement q of the two bipolarons. Both two bipolaron work as partner and form a homopolar binding between the two sites and decrease electronic energy of bipolaron. Here long horizontal arrow showing the light induced transfer of one of the electron of a bipolarons to another neighboring site [24].

As we discussed earlier that the congruent or undoped Lithium Niobate show photorefractive effect which can change the refractive index of Lithium Niobate during operation and effect many applications such frequency conversion , switching and modulation of light etc. and as this process is irreversible , so a proper way need to find which can suppress the photorefractive damages. One solution to this problem is doping of congruent Lithium Niobate with MgO which increase its resistance to photorefractive damage or optical damage. Doping the congruent lithium crystals with Mg above 5 moll % help to remove the NbLi antisites and restrict the formation of both small polarons as well as bipolarons[27]. Doping with the magnesium oxide (MgO) also change the lattice geometry and shift the iron ions (Fe^{+3}) near to conduction band and lessen the effect of the deep traps which restrict the superliner behavior at the infrared wavelength photorefractive damage in the Lithium Niobate sample[25].

1.5.2 Optical properties of MgO doped Lithium Niobate

One of the most important advantage of MgO doping is increment in resistance aginst the photorefractive damage in Lithium Niobate , investigations show that MgO doped LN can stand 1000 time higher intensity of light respective to congruent LN against photorefractive damage[20,27]. Besides this doping of MgO also alter other optical properties of Lithium Niobate. Ordinary and extraordinary refractive index, electro optic coefficients, nonlinearity coefficients etc. . it is investigated that the melting point of LN varies with the doping concentration of MgO and maximum at 5mole% and then decrease with further increment of MgO concentration and maximum mole % of MgO is predicted up to 25%[25].

1.5.2.1 Refractive index.

Refractive index variation is one of the important factor in usability of MgO doped LN, Zelmon, David et. al studied the refractive index variation for 5 mol% doped LN by measuring the dispersion for both congruent and doped sample and determine sellimier's equation coefficients for MgO doped Lithium Niobate[26].

$$n_e^2-1 = A\,\lambda^2/(\lambda^2-B) + C\,\lambda^2/(\lambda^2-D) + E\,\lambda^2/(\lambda^2-F) \quad \ldots\ldots\ldots(1.5.1)$$

Equation (1) is the sellimier's equation used to find the refractive index at different wavelengths.

Table 1.5.2.1.1 sellimier's equation coefficients for congruent Lithium Niobate

Coefficients	Extraordinary refractive index(n_e)	Ordinary refractive index (n_e)
A	2.9804	2.6734
B	0.02047	0.01764
C	0.5981	1.2290
D	0.0666	0.05914
E	8.9543	12.614
F	416.08	474.6

Table 1.5.2.1.2sellimier's equation coefficients for MgO doped Lithium Niobate

Coefficients	Extraordinary refractive index(n_e)	Ordinary refractive index(n_o)
A	2.4272	2.2454
B	0.01478	0.01242
C	1.4617	1.3005
D	0.05612	0.05313
E	9.6536	6.8972
F	371.216	331.33

Calculation of refractive index for ordinary and extraordinary ray of MgO doped Lithium Niobate using the above sellimier's equation and its coefficients show reduction in both in comparison to congruent Lithium Niobate sample. Few year back R.K. Choubey , P. Sen , P.K. Sen et. all reported an experiment measure refractive index for different mol% doping which also show the decrement in both refractive index.

Table 1.5.2.1.3The refractive indices for undoped and MgO doped LN crystals at 532 nm[27]

Sample	Extraordinary refractive index(n_e)	Ordinary refractive index(n_o)	Change(Δn)
undoped	2.3275	2.2329	0.0946
3% Mg-LN	2.2271	2.2096	.0175
5% Mg-LN	2.1841	2.1592	.0249
7% Mg-LN	2.1308	2.1155	.0153

Table 1.5.2.1.4The refractive indices for undoped and MgO doped LN crystals at 1064 nm[27]

Sample	Extraordinary refractive index(n_e)	Ordinary refractive index(n_o)	Change(Δn)
Undoped LN	2.2251	2.1736	0.0515
3% Mg-LN	2.2188	2.1289	.0899
5% Mg-LN	2.2147	2.1260	.0887
7% Mg-LN	2.2116	2.1252	.0864

These table show that for different concentrations of Mg refractive index value decrease which endorse the fact that doping of MgO reduce both ordinary and extraordinary refractive index and change in refractive index also vary with increase the mol% of Mg variation in respect to undoped sample get decrease. In our project we perform experiment at 1330nm and 1550 nm for which calculated values of refractive index using the above sellimier's equation and its coefficients are respectively 2.136 and 2.139.

1.5.2.2 Electro optic coefficient

This is well known that a small concentrations of MgO (>5%) reduces the problem of photorefractive damage efficiently. But if we have to use device for electro optic modulation or switching it's also important to study the effect of MgO doping on electro optic coefficient Lithium Niobate crystal. Most recently Wan-Ying Du, Zi-Bo Zhang et all reported experimental study to determine EO coefficient for MgO doped Lithium Niobate for different Li_2O concentration results are shown in table

Table 1.5.2.2.1effect of MgO doping on electrooptic coefficients of Lithium Niobate[28]

Li_2O content (mol. %)	γ13 (pm/V)	γ33 (pm/V)
43.4	10.5(10.1)	34(32.73)

43.6	10.2(9.8)	33.3(31.9)
43.9	9.8(9.5)	32.4(31)
44.2	10.4(9.2)	31.6(30.3)
44.5	9.2(8.9)	30.6(29.6)

Table showing the variation of electrooptic coefficients with respect to congruent LN sample. It's clear from the table that doping of MgO for different Li_2O mol% increase both electrooptic coefficients (γ13&γ33) and increment is respectively around 14% for γ13 and around 11% for γ33

CHAPTER 2

2. Optical waveguide modulator

2.1 Mache Zehender interferometer

Mache zehender interferometer is a device basically used in physics to measure relative change in phase shift between two collimated rays generated by splitting a single a ray, phase shift may arise due to change in travelling media or due to change in path length of both rays[29].

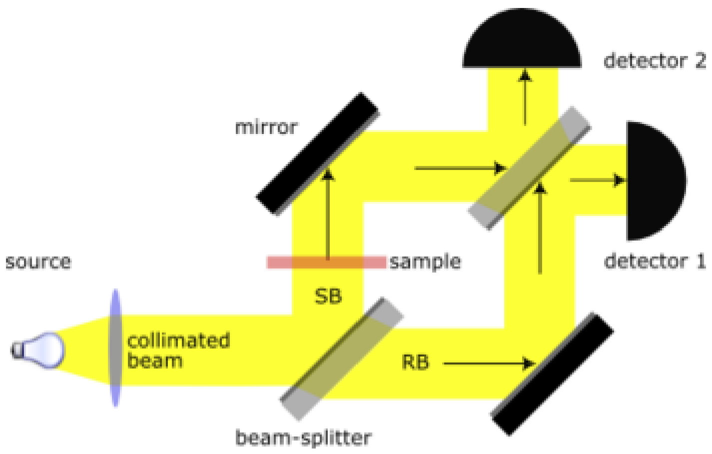

Figure 1.5.2.1 Mache zehender interferometer[30]

In this scheme a collimated ray is originated from a source splits in two parts by reflecting half and refracting other half using a beam splitter which in nothing but a “half silvered ” mirror or a crummy mirror. After this both ray travel through different media and through different path and goes through different phase shift, again these two beams collimated at detector and form constructive or destructive interference or something in between of them if phase difference is between 0 and 180 degree, we can adjust the both path length to get exact 0 or 180 degree phase shift [30].

$$\delta\emptyset = \frac{2\pi}{\lambda} n.\Delta l \qquad \text{........(2.1.1)}$$

Here $\delta\emptyset$ is relative phase shift of both rays again collimating at detector and Δl is path difference between both rays before meeting at detector , λ is wavelength and n is the refractive index of media , this equation is used when refractive index of both media is same but path length is different. If refractive index of both medium is different and path length is equal then phase difference can be measure using of this equation instead equation (1).

$$\delta\emptyset = \frac{2\pi}{\lambda} \Delta n. l \qquad \text{………(2.1.2)}$$

2.2 MZI electrooptic modulator

Basic principle of MZI modulator is same as discussed above the only difference is that here phase variation is cause due to applied voltage on optical signal carrying arms]and because of electro optic effect refractive index of media change slightly and it creates phase difference[31]

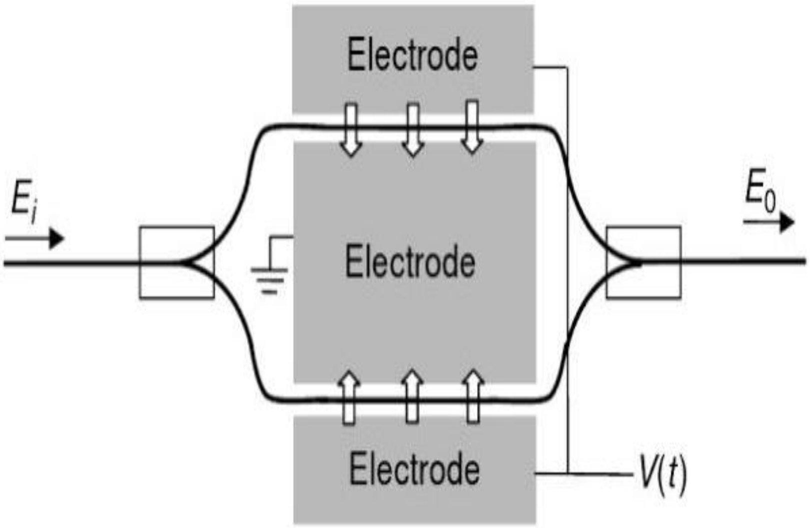

Figure 1.5.2.1MZI electrooptic modulator[32]

As depicted in above figure optical signal is launched from IN port and splits in two equal parts as it goes through 3dB coupler, as both arm are same in length and have same refractive index so no chance of relative phase shift between both. But if we apply some voltage at any one of arm or both arms the refractive index of one or both change due to electrooptic effect according to applied voltage bias and corresponding phase shift occurs. Sometimes only single arm used to apply electrical signal and sometimes both arm used one for dc biasing and other for electrical signal. Both arm’s signal again interact with each other at next coupler , here both signal interface and phase modulation is converted in to intensity modulation and modulated optical signal emerge from OUT port.

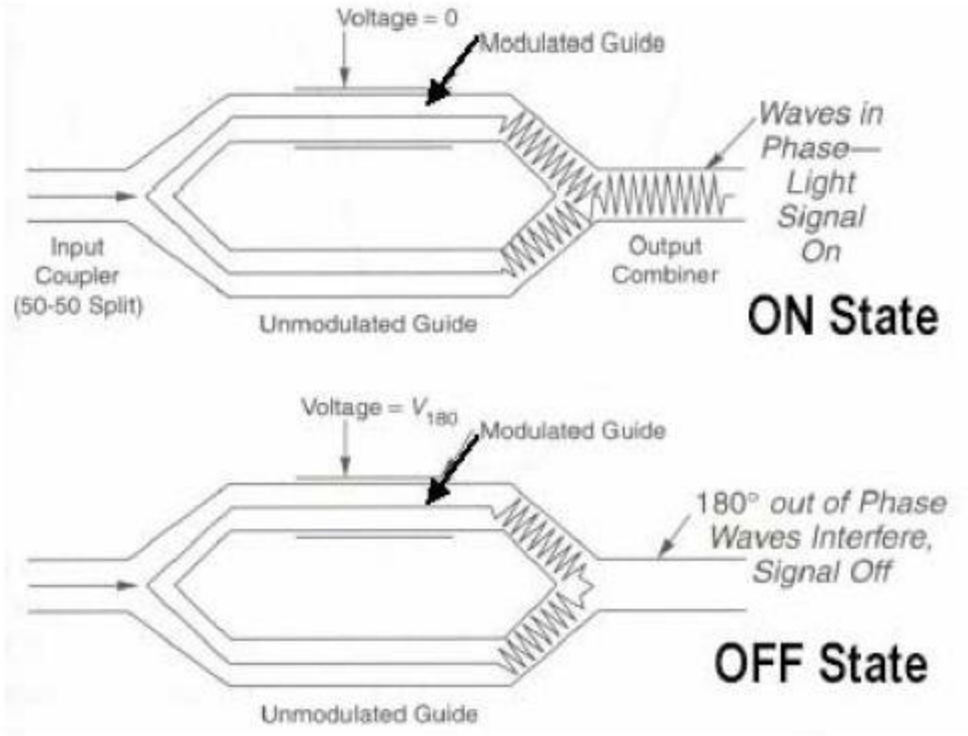

Figure 1.5.2.2MZI modulation scheme[32]

Long-haul transmission of high bit-rates optical signals is mostly based on external modulation technique. The DFB laser is biased at a well-controlled DC bias and temperature, producing a very stable optical power output, both in amplitude and wavelength. The laser's optical output is passed through a separate device that modulates the optical carrier intensity – the external modulator. In this way, the unwanted effects of the direct modulation of the laser are avoided and the quality of the optical signal transmitted enables long-haul transmission over standard SM fibers

There are few types of external modulators described in the literature loss modulator, directional coupler modulator, total internal reflection modulator and Mach-Zehender modulator, the last one being one of the most popular external modulators used. This report summarizes the theoretical background, description and results of an experiment conducted in the Optical Communications and Applied Photonics .

Mache zehender interferometer can be operated in two configurations

(1) symmetric push pull configuration (2)asymmetric configuration

2.2.1 Symmetric push pull MZI

If we apply a certain data and voltage supply V volt at one arm while inverted data and supply voltage at remaining second it's call MZI push pull or MZI symmetric configuration[75] .it means

$$V_1 = -V_2 \quad \ldots\ldots\ldots\ldots\ldots\ldots\ldots(2.2.1)$$

This scheme introduce equal and opposite phase shift in each arm and thus increase the relative phase difference between both.

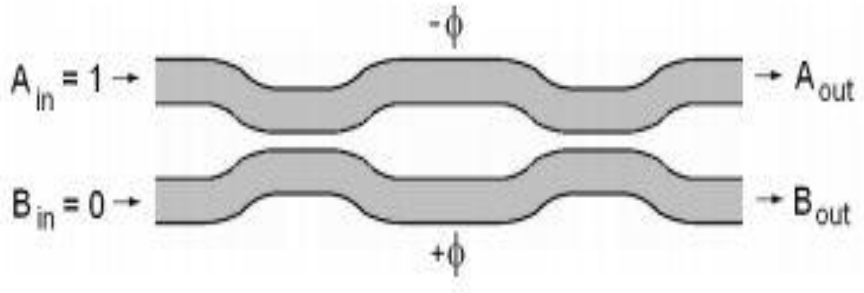

Figure 2.2.1.1MZI push pull or symmetric configuration

2.2.2 Asymmetric configuration

In this scheme RF voltage either apply with single arm or if with both arm is used then one for dc biasing and other for voltage signal. In this project we are using asymmetric MZI configuration for modulation.

Let P_{in} is the total input power from IN port, and P_o is the output power from the OUT port. Let P1 and P2 is the power through each arm of MZI after passing through 3dB coupler and $\Delta\emptyset$ is the relative phase difference between P1 and P2 due to electrooptic effect when they meet again, so light intensity at OUT port will be proportional to [31]

$$P_o^2 = P_1^2 + P_2^2 + 2 P_1 P_2 \cos\Delta\emptyset \ldots\ldots\ldots\ldots\ldots\ldots(2.2.2)$$

$$\Delta\beta = (2\pi/\lambda)\,\Delta n = (2\pi/\lambda) n^3 r\, V/d \ldots\ldots\ldots\ldots\, (2.2.3)$$

where Δn change in refractive index due to applied voltage, n is the refractive index of MZI arm , r is the electrooptic coefficient , V is applied voltage , d is the separation between electrode

$$\mathrm{Eout} = \frac{\mathrm{Ein}}{2}\,\mathrm{e}^{j\beta 1 l} + \frac{\mathrm{Ein}}{2}\,\mathrm{e}^{j\beta 2 l} \ldots\ldots\ldots\ldots\ldots\ldots (2.2.4)$$

$$\mathrm{Po} = \mathrm{Pincos}(\Delta\beta l)\mathrm{e}^{j\beta'' l} \ldots\ldots\ldots\ldots\ldots\ldots\ldots.. (2.2.5)$$

Where $\Delta\beta = (\beta 1 - \beta 2)/2$ and $\beta'' = (\beta 1 + \beta 2)/2$

β1 and β2 represent the phase constant of respectively first and second arm of MZI.

Here equation (2) represent the intensity modulated optical signal outputof input optical signal in which cosine term responsible for intensity of optical output signal at OUT port while exponential stand for time dependent variation of phase. The biggest advantage of MZI modulator is that if we apply equal but opposite polarity voltage on MZI arms then β” =0 and phase term get eliminated completely and output is a pure intensity modulated signal. So the output optical signal intensity will be proportional to multiplication of input intensity and the cosine terms which depend on relative phase shift between both arm signals.

$$\frac{\mathrm{Pout}}{\mathrm{Pin}} = \frac{|\mathrm{Eout}|2}{|\mathrm{Ein}|2} = A\cos 2(\Delta\beta l) \ldots\ldots\ldots\ldots\ldots (2.2.6)$$

$$\frac{\mathrm{Pout}}{\mathrm{Pin}} = A\cos 2\left(\frac{\pi \mathrm{Vm}}{2\mathrm{V}\pi}\right) \quad \ldots\ldots\ldots\ldots\ldots\ldots\ldots (2.2.7)$$

Where V_m is the modulating voltage and V_π is the voltage required for 180 degree relative phase shift.

Modulation voltage for the structure can be calculated theoretically using the following formula[8]

$$V_\pi = d\ \lambda/2\ r_{33} n_e^3 L\zeta \qquad \ldots\ldots\ldots\ldots..(2.2.8)$$

Where d is the separation distance between signal and ground electrode, λ is operating wavelength, r_{33} is electro-optic coefficient of MgO-LN, n_e is the refractive index of extraordinary ray travel in thin film, L is length of electrode (4000 µm) and ζ is the optical confinement factor inside MgO-LN film

2.3 Ridge waveguide modulator

Electrooptic modulator using the ridge waveguide structure have numerous advantage over the conventional waveguide formation technique i.e. ease of fabrication , moderate refractive index profile , better mode confinement etc. it is constructed by depositing a narrow strip ridge over a two dimensional electrooptic or dielectric material slab.

2.3.1 Basic principal of optical waveguide

Figure 2 showing the simplest two dimensional structure of optical waveguide in which core where optical signal travel is sandwiched between two dielectric layers of low refractive index cladding and substrate. Optical field confinement depend on refractive index contrast of core with substrate and cladding , here signal traveling in X-Z plane but it can scatter in y direction also.

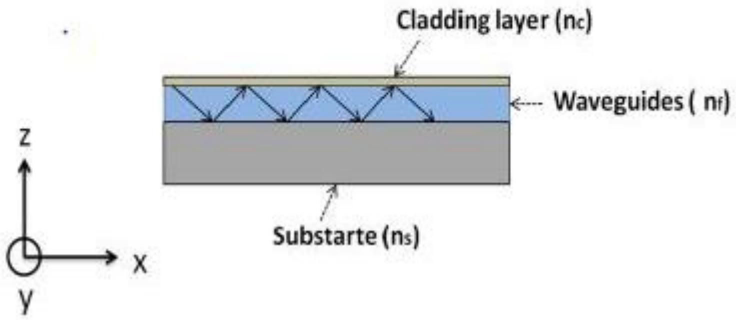

Figure 2.3.1.1planar optical waveguide

Basic principal of operation of optical waveguide is also total internal reflection: light get reflect back when it travel denser (core) to sparse (cladding or substrate) medium. In optical waveguide to match the condition of total internal reflection refractive index of substrate and cladding is kept below the refractive index of core. Generally refractive index found in this manner

$$n_C < n_S < n_S$$

figure 3 showing the structure of ridge waveguide which is quite similar to simplest planar optical waveguide the only difference is that here core is not completely cover by low refractive index layer just only a ridge constructed over the core to confine the optical field inside core. Dimension of ridge along the dimension of core play an important role in mode confinement. As only just some part of core is covered by ridge and rest is open so air work as cladding or we can use any other material for cladding.

Figure 4 is showing the typical refractive index distribution which show that in ridge waveguide core have highest refractive index and substrate and ridge reside with lower refractive index while by default cladding is air so it have lowest refractive index. In ridge waveguide we can use either same or different material for ridge and substra**te.**

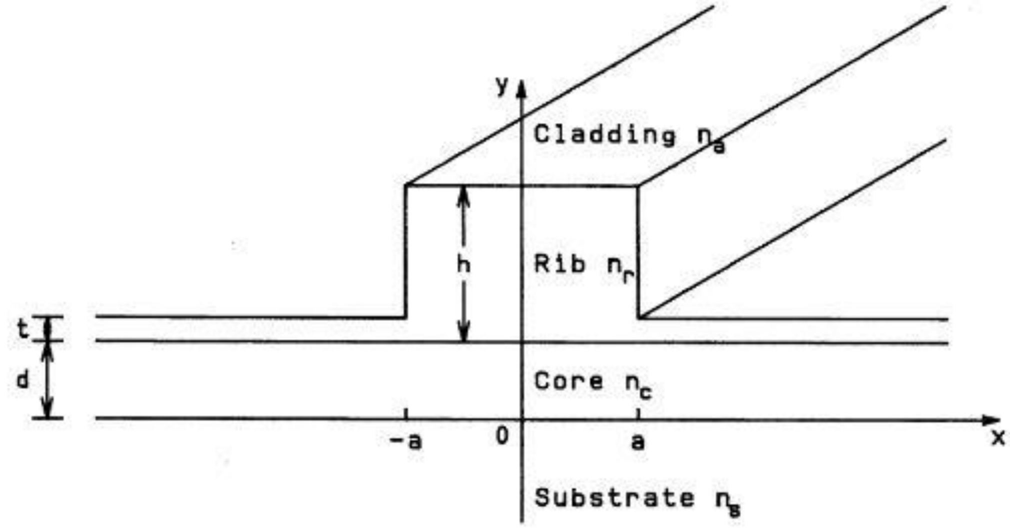

Figure 2.3.1.2 ridge waveguide structure[8]

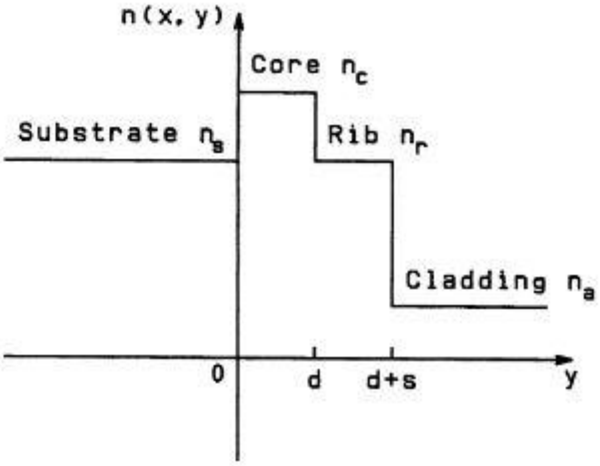

Figure 2.3.1.3 typical refractive index distribution of ridge waveguide [8]

2.3.2 Design rules for ridge waveguide

While designing a ridge waveguide modulator it is important to select dimension of core and ridge in such a manner that it can confine optical field strongly inside the and remain single mode. It is important to study the behavior of waveguide according to dimensions of ridge and core, for this purpose Soref et.al first proposed a equation to keep ridge waveguide showing in figure 5 as single mode waveguide[33]

$$\frac{W}{H} \leq 0.3 + \frac{r}{\sqrt[2]{1-r2}} \ldots\ldots\ldots\ldots\ldots\ldots(2.3.1)$$

Where $r = \frac{h}{H}$

Valid for r ranging 0.5 to 1.

Where W is total width of ridge H is sum of thickness of core and ridge and r is ratio of ridge height to total thickness.

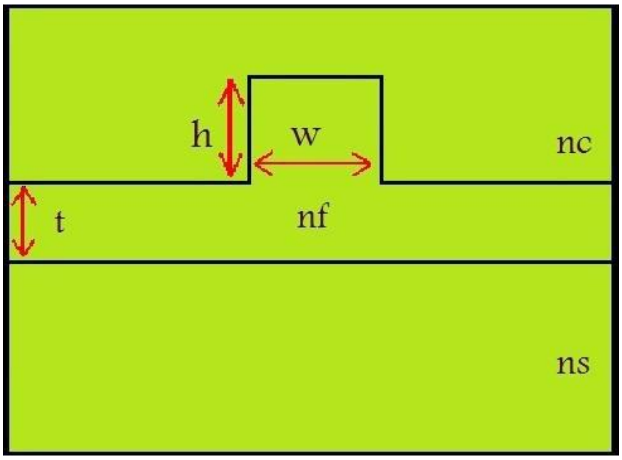

Figure 2.3.2.1 cross section of ridge wave guide

Equation(1) is valid only for relatively larger size rid waveguide and for single mode operation assume that if we consider dimensions according to equation(1) then these get coupled to outer slab or cladding.

Chan et al. produce an equation to predict the dimension for relative small ridge waveguide to operate as a single mode and polarization independent [34].

$$\frac{W}{H} \leq 0.05 + \frac{(0.94+0.25H)r}{\sqrt[2]{1-r2}} \qquad \ldots\ldots.(2.3.2)$$

For $0 \leq r \leq 0.5$ and $1 \leq H \leq 1.5$

2.3.3 Ridge waveguide MZI modulator

Figure showing a typical diagram of MZI modulator using ridge waveguide structure. First a thin film og MgO doped Lithium Niobate is deposited over a substrate the a modulator structure is constructed using ridge material. As depicted as soon as signal launched in device first it get splits in two equal parts due to 3dB coupler stricter then both part travel through MZI arms. One arm of MZI excited using electrooptic, electro absorption, acoustic optic effect or by any other mean which causes a phase shift in core material. After travelling through MZI arm when both signal again meet they form constructive or destructive interference depended upon relative shift between them and results intensity modulated optical output signal.

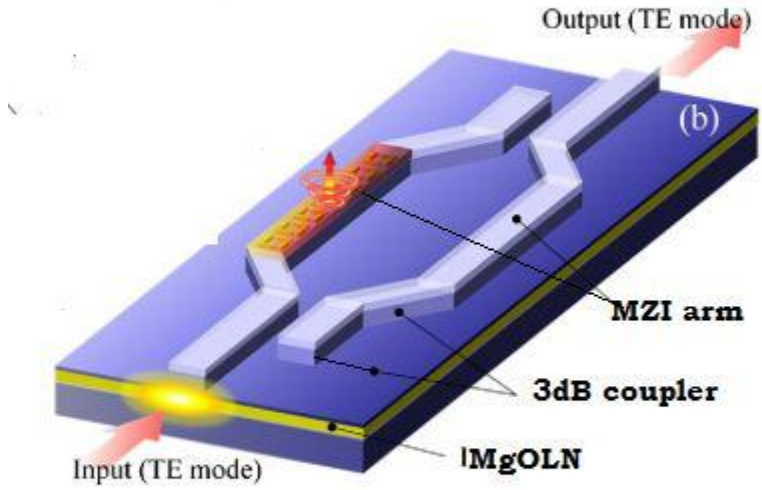

Figure 2.3.3.1ridge waveguide MZI modulator

CHAPTETR 3

3. Simulation and Conclusion

3.1 Simulation method and tools

Simulation of the current project is accomplished using the OptiBPM software which is a comprehensive CAD tool used to design of optical waveguide structures. It is a powerful, handy and friendly software simulation platform which allows us to simulate various integrated and fiber optics guided structure on our system. We can simulate the waveguide structure in both 2-D and 3-D as per our requirement.

The 2-D dimensions are

• X-direction (vertical)—Transverse

• Z-direction (horizontal)—Propagation

The 3D dimensions are:

• X-direction (vertical)—Transverse

• Y-direction—Depth

• Z-direction (horizontal)—Propagation

This simulation tool use beam propagation method (BPM) which is an approximation technique to observe the propagation of optical signal in slowly varying optical waveguide structure [35]. BPM is a numerical method mostly used to simulate and observe the guided optical signal propagation in inhomogeneous media , since 1980's it is used to analysis all kind of waveguide structure for example tapers, Y junction, bends[36] , electrooptic modulators, grating[37], couplers etc. It also solve the Maxwell's equation using the finite difference method rather than solving partial differential equations so also known as FFT-BPM. This method simulate the structure consider some assumptions which are as-

First assumption is that the phase error in transverse direction is very small and it cannot be applied to structure having larger index discontinuities.

(1) A paraxial approximation is made that means it gives accurate results only when beam propagate in the direction of optical axis or nearly in the direction of the optical axis.

(2) This method describes only scalar behavior of the signal so it cannot be applied to analyze the vector properties eg. Polarization dependence and polarization coupling etc.

(3) It completely work in frequency domain so only weak nonlinearities can be modeled using this method.

3.2 Defining the materials

To create the waveguide structure in OptiBPM simulation software first we have to define the material which we are going to use for project. First open the OptiBPM designer and chose a new project an initial properties dialog box appear as shown in figure 1. From this clicking on profile and material tab guide to profile designer layout where we can define the materials.

Here we define the substrate, insulator, cladding, ridge and electrode material by inserting the proper value of their attributes. From the directory under the material folder select the dielectric and chose new and store this with following attributes

table 3.2:1 dielectric material attruibutes

Name	Refractive index at 1330nm	Refractive index at 1550nm	Horizontal EO coefficient(r_H)	Vertical EO coefficient (r_v)
MgO LN	2.136	2.129929	34.6	0
SiO_2(silicon dioxide)	1.44	1.44	0	0
Si_3N_4(silicon nitride)	1.9	1.9	3.02	0.86
air	1	1	0	0

After defining the dielectric material we have to create electrode materials used to apply RF signal for external modulation. Select the new from electrode folder available in profile designer layout and store them with following attributes

Table 3.2.2 electrode material attributes

Name	Refractive index at 1330nm	Refractive index at 1559nm	Horizontal EO coefficient(r_H)	Vertical EO coefficient (r_v)
Signal electrode	1.6	1.6	-	-
Ground electrode	1.6	1.6	-	-

After defining the dielectric materials with their properties that we are going to use to simulate the modulator layout next part is to create the channel profile and that we create by right clicking the profile folder and then select a new profile to store in profile designer window and store it following attributes

Table 3.2.1 channel profile attributes

Profile name	2 D profile definition	3 D profile definition					
	Material	Width (µm)	Thickness (µm)	Offset	Material	Left slant angle	Right slant angle
ridge_wg	Si_3N_4 (silicon nitride)	3	0.3	0	Si_3N_4 (silicon nitride)	90	90

Signal electrode_wg	Signal electrode	2	0.2	0	signal electrode	90	90
Ground electrode_wg	Ground electrode	2	0.2	0	ground electrode	90	90

Here we reached at the completion of material defining part and move on to layout designing part.

3.3 Layout design

As soon as we move back to OptiBPM designer window we have a pop up window in which we have to insert some default value and some initial dimensions for layout. So store the different sections of pop upped window with following attributes

Default waveguide:

Waveguide default width : 4um

Waveguide default profile: ridge_wg

Wafer dimensions

Length : 10000um

Width : 40um

2 D wafer properties

Material : SiO_2 (silicon dioxide)

3 D wafer properties

Cladding

Material : SiO_2 (silicon dioxide)

Thickness : 4um

Substrate

Material : air

Thickness: 1um

After storing these initial and default values of waveguide next part is to draw the layout for project with the help of different shapes of waveguides available in OptiBPM designer tool bar. But before drawing the ridge we have to draw remaining layer of modulator such as insulator layer and then thin film layer of MgO-LN. so choose *draw->regions->substrate region* from toolbar available in OptiBPM layout designer window. As soon as we click on substrate region option a pop up window to draw layers get open and by inserting values for different attributes we draw requiting layers of modulator.

Substrate region

Name : region substrate1

Z position :

Start offset : 0

End offset : 10000

Table 3.3.1 substrate layer attributes

Serial no of layer	Starting thickness (µm)	End thickness (µm)	Material
1	2	2	SiO_2(silicon dioxide)
2	0.73	0.73	MgO LN

This will draw the required layer for modulator and now we can draw our ridge structure over the layers drowned recently. Ridge structure is developed here by using the different waveguide structure available in tool bar like linear, s bend etc.

Table 3.3.2 electrode dimensions

Label	Horizontal start offset (µm)	Horizontal end offset (µm)	Horizontal end offset (µm)	Vertical end offset (µm)	Width (µm)	Depth (µm)

Linear 5	3000	13	7000	13	2	2.73
Linear 6	3000	7	7000	7	2	2.73

Table 3.3.32 waveguide layout dimensions

Label	Horizontal start offset (µm)	Vertical start offset (µm)	Horizontal end offset (µm)	Vertical start offset (µm)	Width (µm)	Depth (µm)
S bend sine1	0	10	1500	3	3	2.73
S bend sine2	1500	3	3000	10	3	0
S bend sine3	0	-10	1500	-2.9	3	2.73
S bend sine4	1500	-2.9	3000	-10	3	2.73
Linear 1	3000	10	5000	10	3	2.73
Linear 2	5000	10	7000	10	3	2.73
Linear 3	3000	-10	5000	-10	3	2.73
Linear 4	5000	-10	7000	-10	3	2.73
S bend sine 5	7000	10	8500	3	3	2.73

S bend sine 6	8500	3	10000	10	3	2.73
S bend sine 7	7000	-10	8500	-2.9	3	2.73
S bend sine 8	8500	-2.9	10000	-10	3	2.73

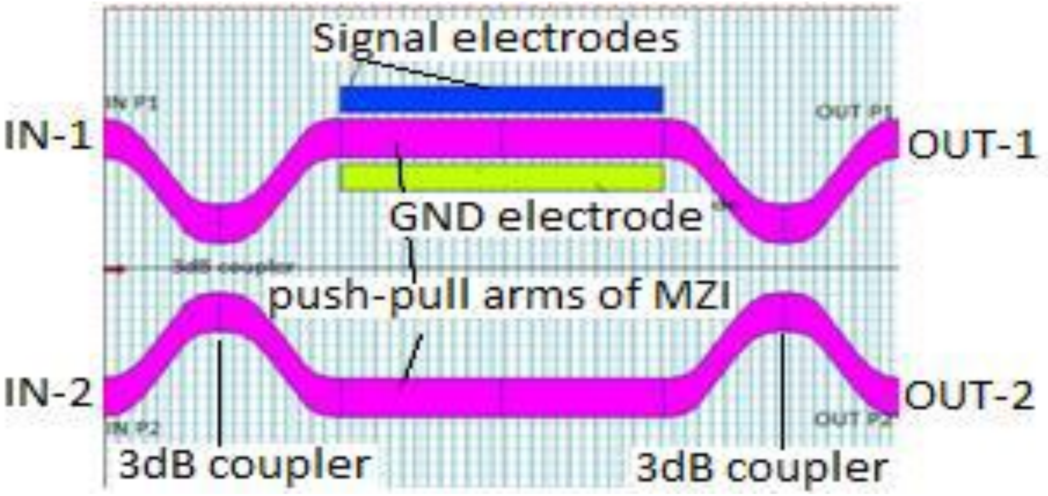

Figure 2.3.3.1 MgO LN MZI modulator layout

These waveguides described above with their attribute complete the structure of MgO-LN all Optical modulator.

Next part of the project is to define an input plane so that we can feed an optical signal in one of the arm of modulator structure. Select *draw* tool from tool bar available in tool bar of layout designer and then select *input plane*

In this and draw it across the structure, it is a red color straight thicker line with an arrow in the middle of it. Now double click on the input plane line set the values of different attributes associated with it.

Input plane

Global data

Starting field : mode

Z position offset : 0

Input field 3D

Click on edit and select a waveguide showing in top right most window and add this to input plane.

From this window we can also calculate the mode using the mode solver and the on solving the mode the structure is found to support single mode with modal index 2.04105062 with semi vectorial TE mode polarization.

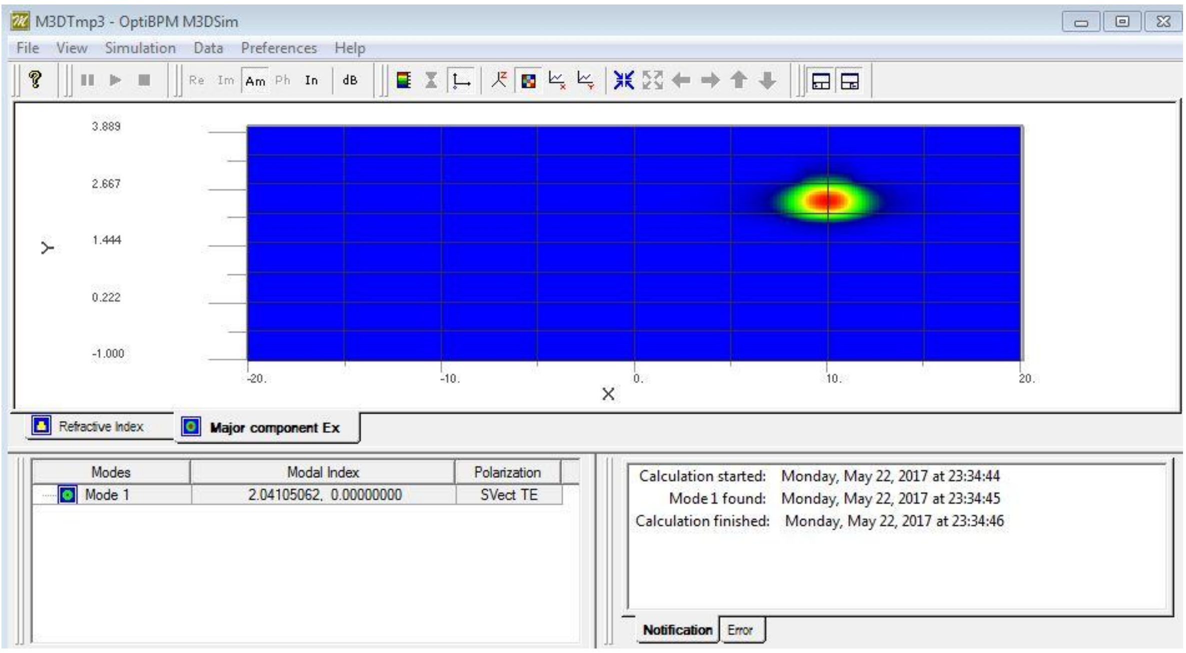

Figure 2.3.3.2mode calculation for waveguide modulator

3.4 Simulation parameter

simulator parameters are the attributes of the simulator software which help in achieve best results of waveguide structure, this include starting field type (modal or Gaussian or any other), wavelength of operation, mesh data, electro optic solver, propagation step, refractive index used by the simulator etc. we can set the simulation parameters by accessing the *simulator* tab available in toolbar of layout designer and further accessing the *simulator parameters* in this.Simulator parameters used for this project are described below.

Global parameters

Starting field : modal

Reference index waveguide : s bend sine 1

Wavelength : 1.33um and 1.55 um(only one at a time)

Number of display : 100

Simulation technique : simulate as is

3 D isotropic

Polarization : semi vectorial TE

Number of point per um in mesh

X→10

Y→27

View cut

X mesh pt→201

Y mesh pt→100

Propagation step : 1.55

Wafer

Width : 40um

Thickness : 5um

Electrooptic simulator : superLU

3.5 Simulation results

Simulation of the current project is done using the OptiBPM simulator 3D version 9 which show the optical power flow in waveguide, refractive index of waveguide along the signal flow and electric field variation under the ridge. Here we can simulate project either for absolute wavelength or for a range of wavelength using the scattering data script generation. After completion of simulation it launch OptiBPM analyser which help to view the simulation results any time and also provide additional data and export of scattering data parameter which are necessary in interfacing of OptiBPM layout designed component in optical circuit using Opti System software platform.

Figure 1 showing the power in waveguide modulator during the simulation of project in which first power is launched in a single port and then divided in two equal parts and undergoes to different phase shift due to electrooptic effect and applied electric field and then again transmitted through a single port. If we change the value of applied voltage then complete power will be transferred from second port. The figure show that the in our layout design everything including 3dB coupler and electrode working perfectly.

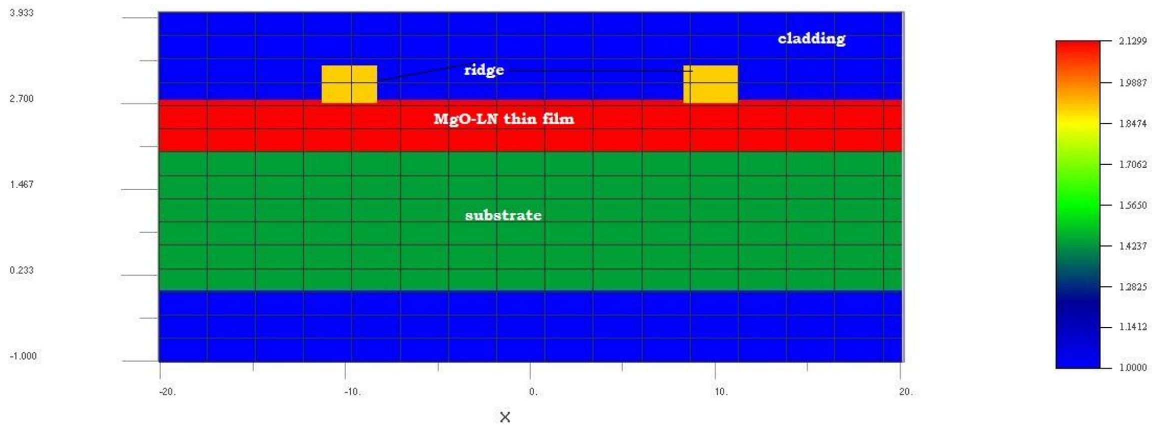

Figure 2.3.3.1 refractive index variation of waveguide with optical signal flow [OptiBPM simulator]

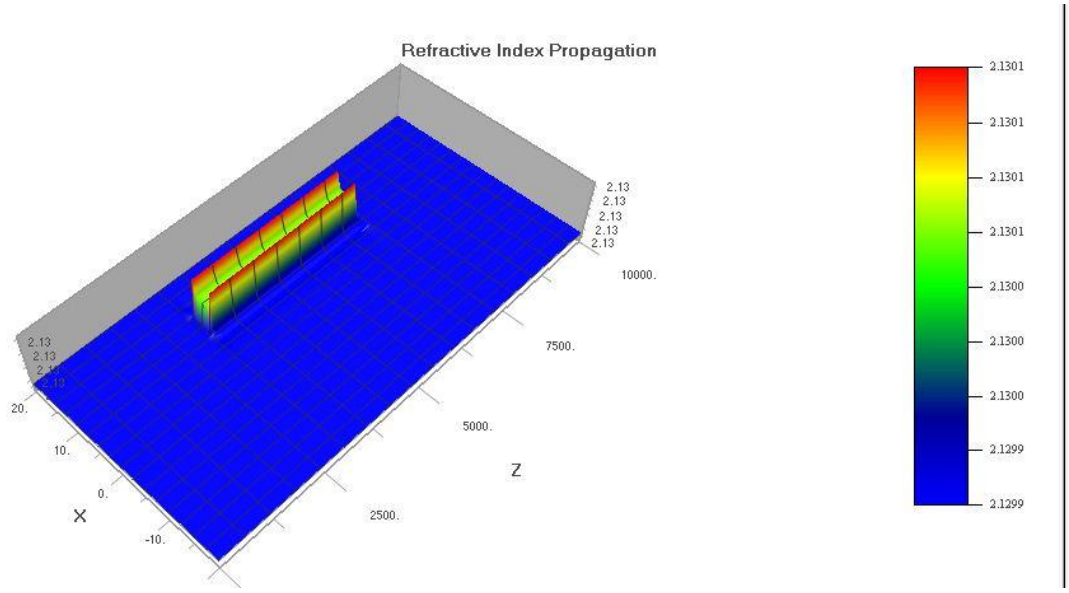

Figure 2.3.3.2 change in refractive index of waveguide due to electrooptic effect 3D view [OptiBPM Analyzer]

Figure 3.5.2, 3.5.3 and 3.5.4 showing the refractive index variation of waveguide. Figure 2 describe the uniformity of refractive index of layout it means when no signal applied refractive index of thin MgO-LN , ridge , substrate layer and cladding is uniform throughout the layout while figure 3 and 4 show variation of refractive index due to electrooptic effect. Whenever optical signal travel through the waveguide modulator and if RF signal or any voltage applied to electrode there is a change occur in refractive index of MgO-LN thin film layer due to the electrooptic effect and this cause relative phase shift in signal of both arms of MZI.

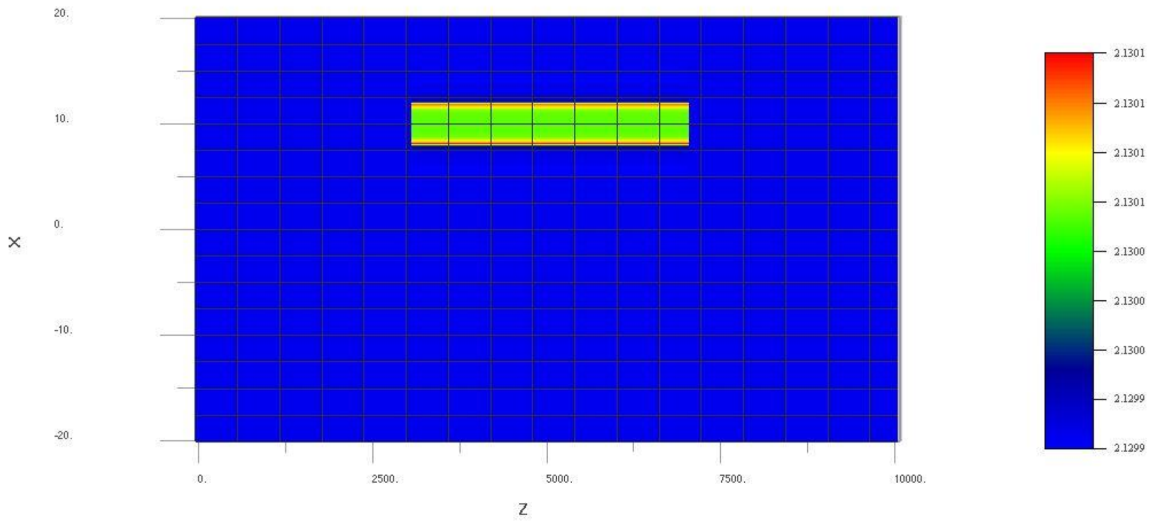

Figure 2.3.3.3 change in refractive index of waveguide due to electrooptic effect 3D view [OptiBPM Analyser]

3.5.1 Mode propagation

Manner or way in which optical signal travel through waveguide is known as mode. As we have discussed in chapter two that mode confinement inside waveguide strongly depend on core and ridge dimension figure 3.5.5 showing the mode propagation inside waveguide for different ridge sizes.

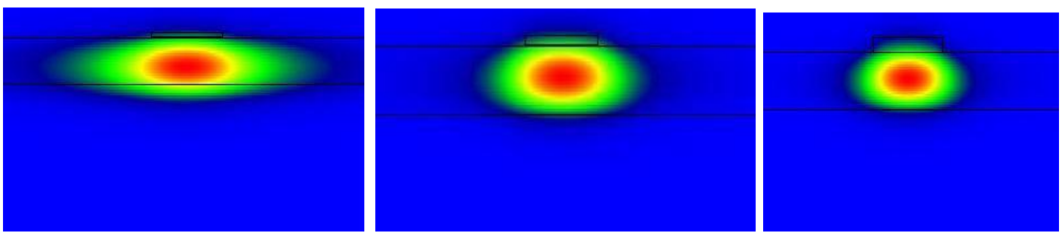

(a) (b) (c)

Figure 3.5.1.1 mode propagation in waveguide for different ridge height (a) h=100nm, (b) h= 200nm, (c) h =300nm, while the width has been kept fixed as w=3μm.

3.5.2 Modulation voltage.

Figure 3.5.5 showing the optical power transmission in two different states which is result of modulation due to applied voltage. Here required modulation voltage (V_π) found 5.5

volt and 6 volt respectively for 1330 nm and 1550 nm wavelength of operation and product of $V_{\pi}L$ found 2.2 v-cm and 2.4 v-cm .

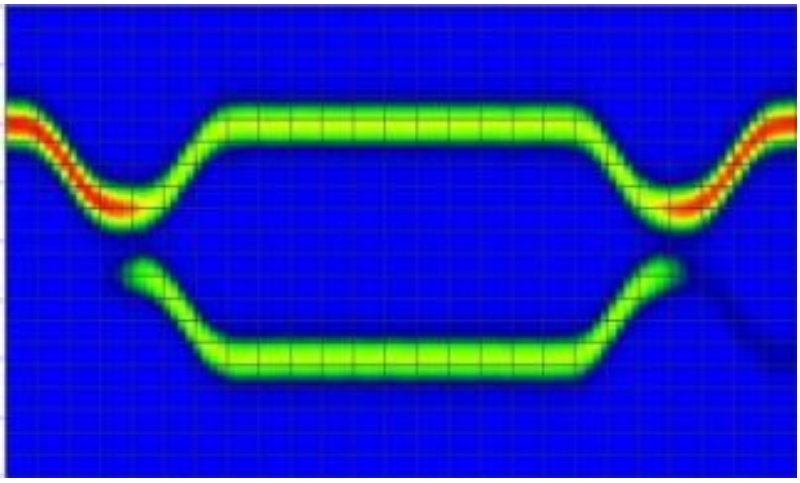

(a)

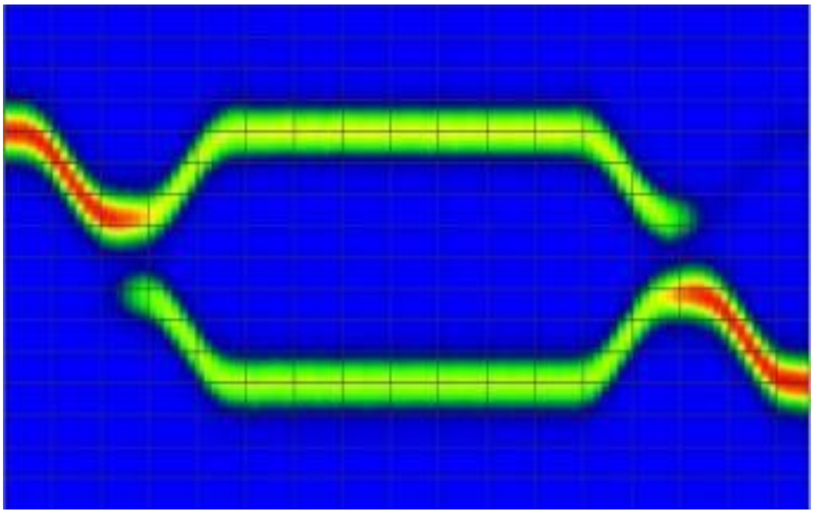

(b)

Figure 3.5.2.1Optical power transmission (a) in BAR mode (b) in CROSS mode

3.5.3 Effect of device parameters

Single mode operation of device is very much important for efficient and long distance communication. In the way to make the waveguide single mode, all the high order modes, must be suppressed or should be below cutoff.These three parameters affect

1.Ridge height

2.Ridge width

3.Core width

3.5.3.1 Effect of Ridge height

Ridge height is mainly responsible for the lateral confinement and reducing the ridge height reduce overall size of device and dominate to poor confinement of mode in lateral direction. Graph depicted in figure showing the variation of effective index versus ridge height, as height of ridge increase effective index also increase but quickly it get saturated and after that it lead to multimode operation of device. On investigating the mode formation in device using BPM mode solver application we can say that if h≤4 μm operation still remains single mode.

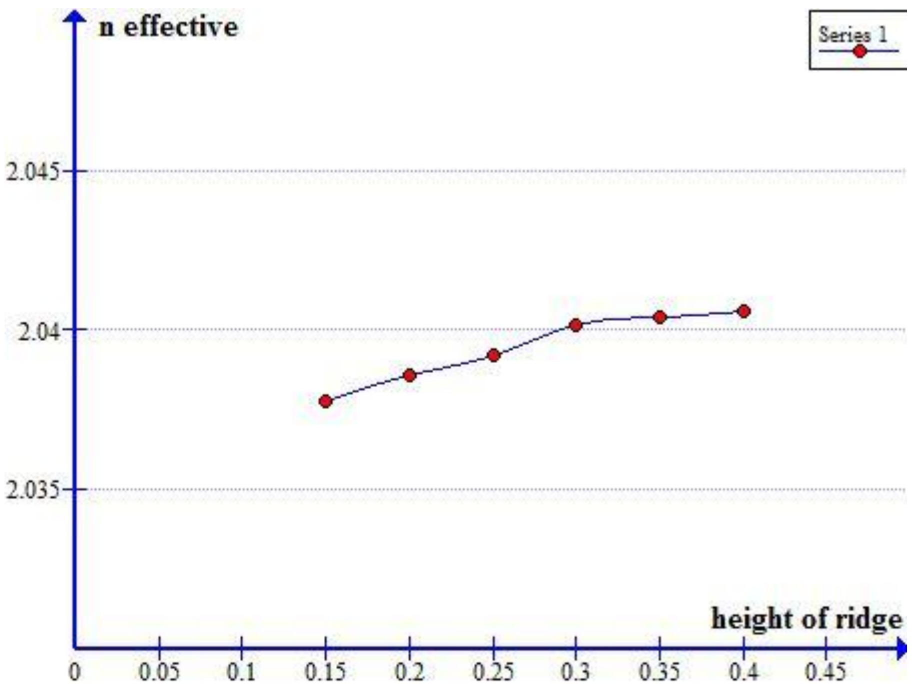

Figure 3.5.3.1effective index v/s height of ridge

3.5.3.2 Effect of ridge width

Waveguide ridge width is also an important parameter, it is responsible for horizontal confinement of mode.it is the only parameter that can be vary easily at time of manufacturing. If we use ridge width of very large then it makes the waveguide multi-mode and if we use waveguide with very narrow ridge dimension then leakage of dominant mode also increase. Figure showing the mode propagation in waveguide for 1 μm and 4 μm which show that as we increase width of ridge power leakage from core reduces but it remains single mode only for w≤ 5 μm

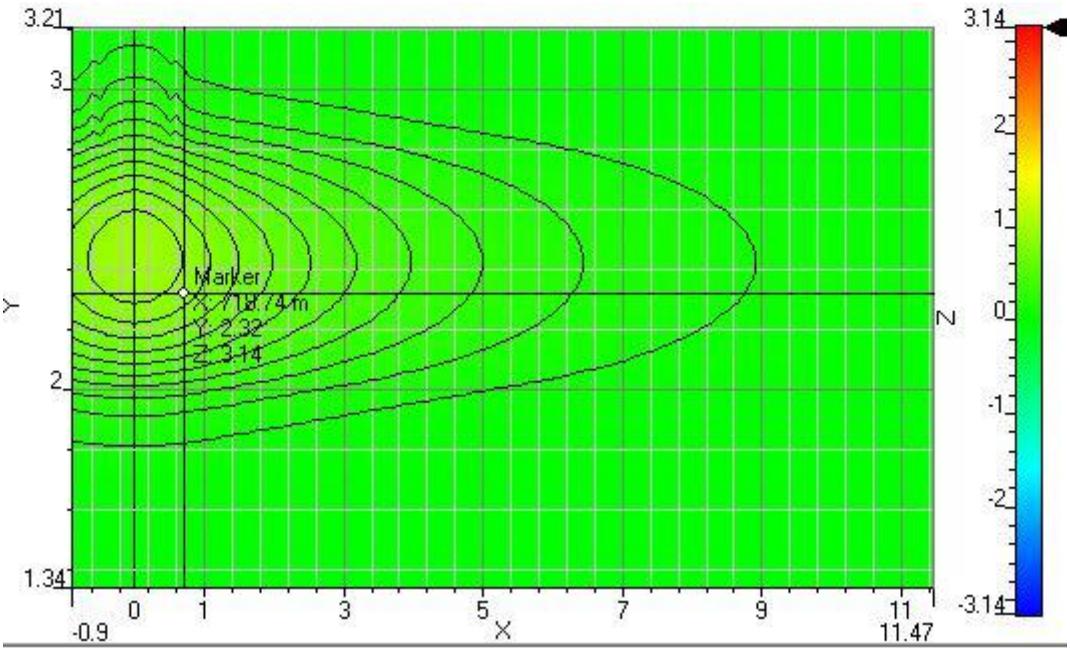

Figure 3.5.3.2cute view of mode propagation for 1 um width

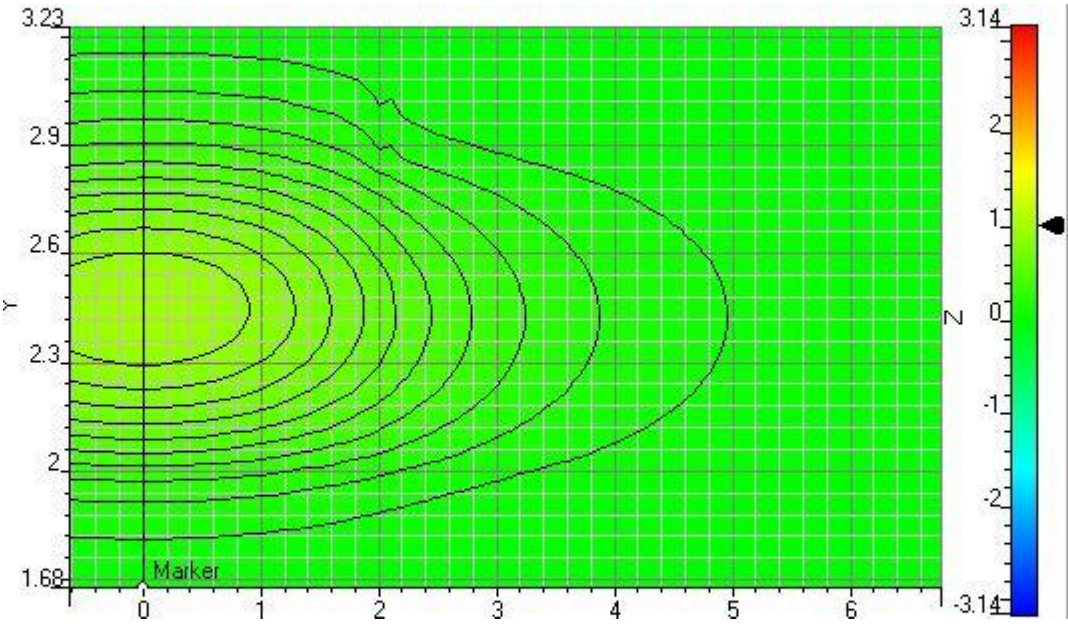

Figure 3.5.3.3cute of mode propagation for 4 um width

3.5.3.3 Effect of core thickness

Although increasing core thickness is another method but it is not desirable. Due to practical reasons. A thick core has a lot of side effects, such as higher thresholds for lasers, and introduces poorer saturation characteristics for a Semiconductor optical amplifier. Figure showing the variation of effective index with core thickness which showing that increasing the core thickness also increase the effective index and hence reduce leakage outside core.

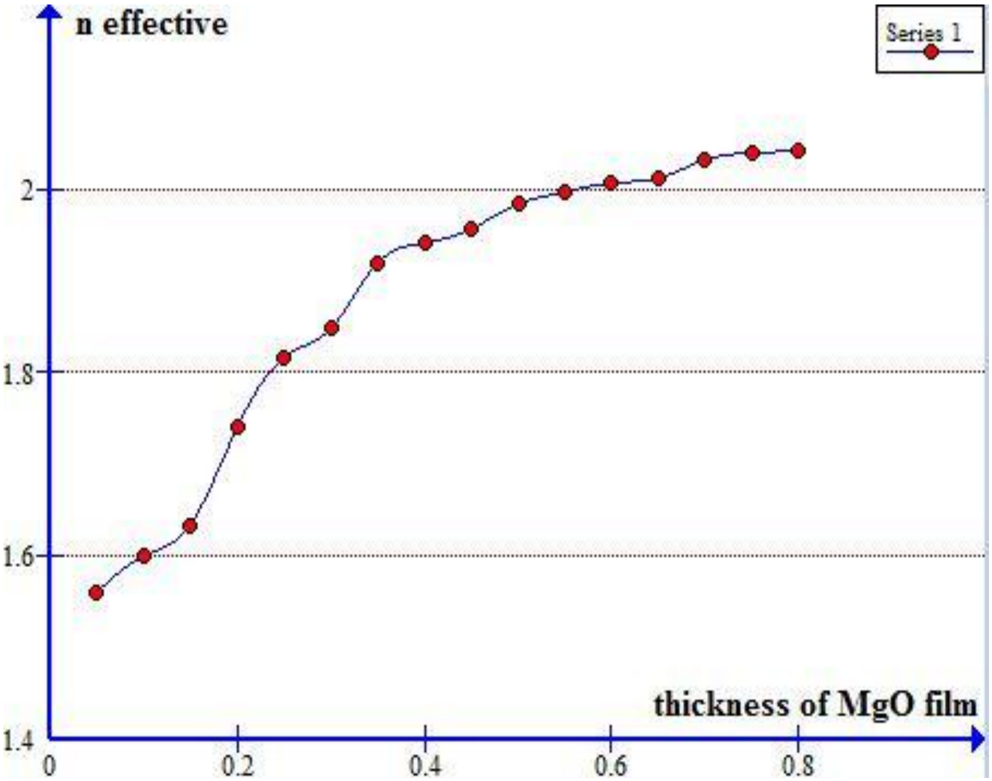

Figure 3.5.3.4effective index v/s core thickness

3.6 Conclusions

- $V_{\pi}L$ for an all optical modulator based on MgO doped LN ridge waveguides for its operation with wavelengths 1550nm and 1330nm are calculated as 2.4v.cm and 2.2v.cm respectively. A comparison of the project structure with different waveguide modulator structure is shown by table

Table 3.6.1 Comparison of results of modulator based on different structures/waveguides

Waveguides	$V_{\pi}L$(v.cm)	Extinction ratio(dB)
MgO-LN(λ=1330nm)	2.2	18

MgO-LN (λ=1550nm)	2.4	15
Si3N4/LN [19]	3	13
Ta2O5 /LN film [38]	4	20
A-Si/LN [39]	8.8	20
ChG/Si/LN [40]	3.8	13

The values reported here are promising as compared to other type of structures; however these results are obtained using OptiBPM simulator software therefore further improvements can be achieved by redefining the MgO doped LN channel waveguide structure.

- Doping of MgO also suppress the "optical damage" effect that means the same structure can also be use for optical switching.
- For the investigated device parameters waveguide operate under signle mode condition satisfactory.

References

[1] Wooten, E.L., Kissa, K.M., Yi-Yan, A., Murphy, E.J., Lafaw, D.A., Hallemeier, P.F., Maack, D., Attanasio, D.V., Fritz, D.J., McBrien, G.J. and Bossi, D.E., 2000. A review of lithium niobate modulators for fiber-optic communications systems. *IEEE Journal of selected topics in Quantum Electronics*, *6*(1), pp.69-82

[2] Weis, R.S. and Gaylord, T.K., 1985. Lithium niobate: summary of physical properties and crystal structure. *Applied Physics A: Materials Science & Processing*, *37*(4), pp.191-203

[3] Abrahams, S.C., Reddy, J.M. and Bernstein, J.L., 1966. Ferroelectric lithium niobate. 3. Single crystal X-ray diffraction study at 24 C. *Journal of Physics and Chemistry of Solids*, *27*(6-7), pp.997-1012

[4] Kitamura, K., Yamamoto, J.K., Iyi, N., Kirnura, S. and Hayashi, T., 1992. Stoichiometric LiNbO3 single crystal growth by double crucible Czochralski method using automatic powder supply system. *Journal of crystal growth*, *116*(3-4), pp.327-332

[5] *Fundamentals of Photonics* Bahaa E. A. Saleh, Malvin Carl Teich 1991 John Wiley & Sons, Inc

[6] Lenzo, P.V., Spencer, E.G. and Nassau, K., 1966. Electro-optic coefficients in single-domain ferroelectric lithium niobate. *JOSA*, *56*(5), pp.633-635.

[7] Jiang, Y., Wang, K.M., Wang, X.L., Chen, F., Jia, C.L., Wang, L., Jiao, Y. and Lu, F., 2007. Model of refractive-index changes in lithium niobate waveguides fabricated by ion implantation. *Physical Review B*, *75*(19), p.195101.

[8] Yariv, A. and Yeh, P., 2007. *Photonics: optical electronics in modern communications* (Vol. 6). New York: oxford university press

[9] Beam propagation method : Technical background and tutorials : Waveguide optics modeling software system, Version 8.0, second edition, Optiwave Inc., 2006.

[10] Peña-Rodríguez, O., Olivares, J., Carrascosa, M., García-Cabañes, Á., Rivera, A. and Agulló-López, F., 2012. Optical waveguides fabricated by ion implantation/irradiation: A review. *Ion Implantation, Prof. Mark Goorsky (Ed.), ISBN*, pp.978-953

[11] Montanari, G.B., De Nicola, P., Sugliani, S., Menin, A., Parini, A., Nubile, A., Bellanca, G., Chiarini, M., Bianconi, M. and Bentini, G.G., 2012. Step-index optical waveguide produced by multi-step ion implantation in LiNbO 3. *Optics express*, *20*(4), pp.4444-4453

[12] [29] Peithmann, K., Zamani-Meymian, M.R., Haaks, M., Maier, K., Andreas, B. and Breunig, I., 2006. Refractive index changes in lithium niobate crystals by high-energy particle radiation. *JOSA B*, *23*(10), pp.2107-2112.

[13] Jackel, J.L., Rice, C.E. and Veselka, J.J., 1982. Proton exchange for high-index waveguides in LiNbO3. *Applied Physics Letters*, *41*(7), pp.607-608.

[14] Loni, A., 1987. *An experimental study of proton-exchanged lithium niobate optical waveguides* (Doctoral dissertation,pg no 11-12 University of Glasgow).

[15]] Singh, G., Yadav, R.P. and Janyani, V., 2010. Ti indiffused lithium niobate (Ti: LiNbO3) Mach-Zehnder interferometer all optical switches: a review. INTECH Open Access Publisher.

[17]] Glass, A.M., Kaminow, I.P., Ballman, A.A. and Olson, D.H., 1980. Absorption loss and photorefractive-index changes in Ti: LiNbO 3 crystals and waveguides. *Applied optics*, *19*(2), pp.276-281.

[18] [40] K. Tanaka and T. Suhara : Fabrication of 0.7μm2 Ridge Waveguide in Ion-Sliced LiNbO3 by Proton-Exchange Accelerated Etching : Conference on Lasers and Electro-Optics Pacific Rim, (Optical Society of America, 2015), paper 26I1_5, ISBN: 978-1-4673-7110-0, 2015.

[19] Shilei Jin, Longtao Xu, Haihua Zhang, and Yifei Li : LiNbO3 Thin-Film Modulators Using Silicon Nitride Surface Ridge Waveguides : IEEE photonics technology letters, vol. 28, no. 7, April 1, 2016.

[20] R. K. Choubey, P. Sen, P. K. Sen, et al. "Optical properties of MgO doped LiNbO3 single crystals", Optical Materials 28, 467–472, 2006.

[21]] Schirmer, O.F., Imlau, M., Merschjann, C. and Schoke, B., 2009. Electron small polarons and bipolarons in LiNbO3. *Journal of Physics: Condensed Matter*, *21*(12), p.123201.

[22] Jermann, F. and Otten, J., 1993. Light-induced charge transport in LiNbO 3: Fe at high light intensities. *JOSA B*, *10*(11), pp.2085-2092.

[23]]Nava, G., Minzioni, P., Cristiani, I., Argiolas, N., Bazzan, M., Ciampolillo, M.V., Pozza, G., Sada, C. and Degiorgio, V., 2013. Photorefractive effect at 775 nm in doped lithium niobate crystals. *Applied Physics Letters*, *103*(3), p.031904.

[24] Betts, G.E., O'Donnell, F.J. and Ray, K.G., 1994. Effect of annealing on photorefractive damage in titanium-indiffused LiNbO/sub 3/modulators. *IEEE photonics technology letters*, *6*(2), pp.211-213

[25] Grabmaier, B.C. and Otto, F., 1986. Growth and investigation of MgO-doped LiNbO3. *Journal of Crystal Growth*, *79*(1-3), pp.682-688.

[26]] Edwards, G.J. and Lawrence, M., 1984. A temperature-dependent dispersion equation for congruently grown lithium niobate. *Optical and Quantum Electronics*, *16*(4), pp.373-375.

[27] David E. Zelmon and David L. Small : Grown Lithium Niobate and 5 mol. % Magnesium Oxide–doped Lithium Niobate: vol. 14, no. 12/December 1997/J. Opt. Soc. Am. B (1997).

[28] Du, W.Y., Zhang, Z.B., Ren, S., Wong, W.H., Yu, D.Y., Pun, E.Y.B. and Zhang, D.L., 2016. Note: Electro-optic coefficients of Li-deficient MgO-doped LiNbO3 crystal. *Review of Scientific Instruments*, *87*(9), p.096105.

[29] Röntgen, W.C. and Zehnder, L., 1891. Ueber den Einfluss des Druckes auf die Brechungsexponenten von Wasser, Schwefelkohlenstoff, Benzol, Aethyläther und einigen Alkoholen. *Annalen der Physik*, *280*(9), pp.24-51.

[30] Zetie, K.P., Adams, S.F. and Tocknell, R.M., 2000. How does a Mach-Zehnder interferometer work?. *Physics Education*, *35*(1), p.46.

[31] Ghatak, A.K. and Thyagarajan, K., 1989. *Optical electronics*. Cambridge University Press.

[32]] Hui, R. and O'Sullivan, M., 2009. *Fiber optic measurement techniques*.page no 121, Academic Press.

[33] Milošević, M.M., Matavulj, P.S., Timotijević, B.D., Reed, G.T. and Mashanovich, G.Z., 2008. Design rules for single-mode and polarization-independent silicon-on-insulator rib waveguides using stress engineering. *Journal of Lightwave Technology*, *26*(13), pp.1840-1846.

[34Chan, S.P., Png, C.E., Lim, S.T., Reed, G.T. and Passaro, V.M., 2005. Single-mode and polarization-independent silicon-on-insulator waveguides with small cross section. *Journal of lightwave technology*, *23*(6), p.2103.]

[35] Feit, M.D. and Fleck, J.A., 1980. Computation of mode properties in optical fiber waveguides by a propagating beam method. *Applied Optics*, *19*(7), pp.1154-1164.

[36] Baets, R. and Lagasse, P.E., 1982. Calculation of radiation loss in integrated-optic tapers and Y-junctions. *Applied optics*, *21*(11), pp.1972-1978.

[37] Danielsen, P., 1984. Two-dimensional propagating beam analysis of an electrooptic waveguide modulator. *IEEE journal of quantum electronics*, *20*(9), pp.1093-1097.

[38] P. Rabiei, J. Ma, S. Khan, J. Chiles, and S. Fathpour "Heterogeneous Lithium Niobate Photonics on silicon substrates" Opt. Exp., vol. 21, no. 21, pp. 25573–25581, 2013.

[39] L. Chen, M. G. Wood, and R. M. Reano, "12.5 pm/V hybrid Silicon and Lithium Niobate optical microring resonator with integrated electrodes" Opt. Exp., vol. 21, no. 22, pp. 27003–27010, 2013.

[40] A. Raoet al., "Heterogeneous microring and Mach–Zehnder modulators based on Lithium Niobate and chalcogenide Glasses on Silicon" Opt. Exp., vol. 23, no. 17, pp. 22746–22752, 2015.

Publications

[1] Sanjay Kumar, Ghanshyam Singh, Vijay Janyani et al. "*MgO doped Lithium Niobate waveguides based All Optical Modulator*" at Optical & wireless technology conference 2017.

[2] Sanjay Kumar Sharma, Laxman Kumar, Ghanshyam Singh "*External modulation using Mach Zhendre interferometer (MZI) basics and operation: A Review*" at OSA Young Student Congress 2016.